ARTICLE IN PRESS

Available online at www.sciencedirect.com

ScienceDirect

Journal of Theoretical Biology ▮ (▮▮▮▮) ▮▮▮–▮▮▮

Journal of Theoretical Biology

www.elsevier.com/locate/yjtbi

Ameboid cell motility: A model and inverse problem, with an application to live cell imaging data

Huseyin Coskun[a,*], Yi Li[b,c], Michael A. Mackey[d]

[a]School of Mathematics, University of Minnesota, Minneapolis, MN 55455 USA
[b]Department of Mathematics, University of Iowa, Iowa City, IA 52242, USA
[c]Department of Mathematics, Hunan Normal University, Changsha, PR China
[d]Department of Biomedical Engineering, University of Iowa, Iowa City, IA 52242, USA

Received 3 January 2005; received in revised form 2 July 2006; accepted 5 July 2006

Abstract

In this article a mathematical model for ameboid cell movement is developed using a spring–dashpot system with Newtonian dynamics. The model is based on the facts that the cytoskeleton plays a primary role for cell motility and that the cytoplasm is viscoelastic.

Based on the model, the inverse problem can be posed: if a structure like a spring–dashpot system is embedded into the living cell, what kind of characteristic properties must the structure have in order to reproduce a given movement of the cell? This inverse problem is the primary topic of this paper.

On one side the model mimics some features of the movement, and on the other side, the solution to the inverse problem provides model parameters that give some insight, principally into the mechanical aspect, but also, through qualitative reasoning, into chemical and biophysical aspects of the cell. Moreover, this analysis can be done locally or globally and in different media by using the simplest possible information: positions of the cell and nuclear membranes.

It is shown that the model and solution to the inverse problem for simulated data sets are highly accurate. An application to a set of live cell imaging data obtained from random movements of a human brain tumor cell (U87-MG human glioblastoma cell line) then provides an example of the efficiency of the model, through the solution of its inverse problem, as a way of understanding experimental data.

Keywords: Cell motility; Ameboid movement; Inverse problem; Cancer cell

1. Introduction

Understanding cell motility is crucial in many aspects of biology, especially for medical sciences. The motility of cancer cells is certainly a pre-eminent case which has attracted attention to the subject. It is thought that increase in motility of tumor cells is associated with cancer metastasis. Similar to metastatic cancer, arthritis and neurological birth defects have their roots in cell motility, as do many other diseases. Cell motility is also essential for shaping organs and tissues during development of an embryo, maintenance of tissues, wound healing, white blood cell movement in immune response, and generation of new blood vessels, etc. (see Alberts et al., 2002; Bray, 2001; Chicurel, 2002; Lauffenburger and Horwitz, 1996). Therefore, the ability to control the motility of cells is crucial for causal and rational treatments, whether curative or preventative.

Because of current theoretical development and experimental results (see, for example, Abercrombie, 1980; Bray, 2001; Mitchison and Cramer, 1996), research on ameboid cell motility is focused on a biophysical explanation, called the pull–push model. This process involves protrusion (see, for example, Mogilner and Edelstein-Keshet, 2002; Small, 1989; Theriot and Mitchison, 1991), adhesion (see, for

*Corresponding author. Tel.: +1 612 624 8389; fax: +1 612 626 2017.
E-mail address: coskun@umn.edu (H. Coskun).

0022-5193/$ - see front matter © 2006 Elsevier Ltd. All rights reserved.
doi:10.1016/j.jtbi.2006.07.025

Please cite this article as: Huseyin Coskun et al., Ameboid cell motility: A model and inverse problem, with an application to live cell imaging data, Journal of Theoretical Biology (2006), doi:10.1016/j.jtbi.2006.07.025.

example, Cox and Huttenlocher, 1998; Defilippi et al., 1999; Kaverina et al., 2002), and contraction (see, for example, Bray, 2001; Mitchison and Cramer, 1996) of the cell through the action of the cytoskeleton. Briefly, it is thought that polymerization and bundling of the actin filaments produce directed force to create protrusion at the cell membrane. The protruding site contacts and adheres to the substratum. Activation of the actomyosin complex, with depolymerization and unbundling in some cases, causes contraction at the rear (or near the nucleus) of the cell. The complexity of the living cell makes it very difficult to explain the mechanism of the motion through the use of a simple model. For this reason, physical models are sometimes focused on the simpler forms of living cells (for example, see Mogilner and Verzi's model (2003) for nematode sperm cell movement).

It is a known fact that cytoplasm is viscoelastic. Viscosity varies from one place to another within the cell and therefore the cell is heterogeneous (for example, see Yanai et al., 2004; Caille et al., 2002). Viscoelasticity is addressed widely in the literature, and measurements are obtained using various methods, such as magnetic tweezers (Bausch et al., 1999) or magnetocytometry (Karcher et al., 2003). Additional analysis and review of the viscoelastic properties of the living cell have been given by Marella and Udaykumar (2004), Feneberg and Westphal (2001), Heidemann et al. (1999), MacKintosh (1998), and Yanai et al. (1999).

The models for cell motility proposed in the literature can be divided into two main groups: 'discrete' and 'continuous' models. The protrusion, contraction, and adhesion mechanisms of the biophysical pull–push model with some modifications and the viscoelasticity of living cells allow modeling these processes using classical mechanical means. Therefore, discrete models (for example, see DiMilla et al., 1991; Palsson and Othmer, 2000) in general use discrete units which are composed of springs, dashpots, and contractile elements either in parallel or in series for physical and mathematical formulation of the models. An important class of this kind of model, called tensegrity models, is discussed in a recent paper by Sultan et al. (2004) (see also McGarry et al., 2004). Continuous models (for example, see Coskun, 2006a; Alt and Dembo, 1999; Bottino et al., 2002; Dong and Skalak, 1992; Gracheva and Othmer, 2004; Mogilner et al., 2000; Mogilner and Verzi, 2003; Schmid-Schönbein et al., 1995; Yeung and Evans, 1989), however, use continuum-mechanical tools, fluid dynamics or thermodynamics. Combinations of these two types are also encountered. A nice introduction to these types of models and a discussion of the literature have been given by Gracheva and Othmer (2004).

The Ring Model which is developed in this paper is a 2-D model. It is designed to model single-cell movement on a rigid, planar, and compliant substrate and assumes a variable number n of radial spring–dashpot subunits to describe mechanical properties of the cytoplasm as well as corresponding subunits for cell and nuclear membranes. In that sense although the Ring Model is set up as a discrete model, it differs from the previous discrete models by its high dimensionality, focus, generality, and complexity.

In this article we often use the terms *forward* and *inverse problems*. By the forward problem, we mean finding the position of the cell at any time once an estimated predetermined set of parameters is provided. By the inverse problem, we mean extracting as much information as possible about the biophysical and mechanochemical properties of the cell from the change of location of the cell. The positions of the cell and its components at different time steps are determined by live cell imaging techniques. Given a set of measurements of the movement of the cell, the inverse problem is posed by asking: if a structure like the Ring Model is imposed into the living cell, what kind of characteristic properties must the structure have in order to reproduce the same movement? The models cited above have focused mostly on the forward problem. The major feature of this paper, i.e. the inverse problem and its solution which is studied primarily—but not yet completely—in this paper, has not been addressed in the literature previously. A comprehensive introduction to this new model-based inverse problem formulation and discussion of both discrete and continuum cases can be found in Coskun (2006b).

Briefly, the model is an oversimplified model as a first step towards the development of model-based inverse problems for cell motility. We would like to bring this new approach to the attention of the scientific community, which may lead to different applications being proposed, or use of the approach for problems similar to those we consider in this introductory paper. Applications to different cases would help in the direction of the further justification of the model.

2. The Ring Model

The main goal of the Ring Model is to develop a method that approximates global or local mechanical characteristics of a crawling cell, so that it may stimulate new physical and biological experiments, or may be used to test the existing measurements. Since the mechanism of cell motility is far too complicated and the experiments are expensive, a quantitative modeling approach that can be analysed under different assumptions is necessary to help in extracting biophysical and chemical insights from the measurements. The model developed here uses the simplest information available: the positions of the cell and nuclear membranes.

2.1. Setup and use of the model

A subunit of the model is defined to be a Voigt solid element, which simply is a spring and a dashpot in parallel. The cytoplasm is modeled as consisting of a fixed number, n, of uniformly distributed subunits radiating from the

Please cite this article as: Huseyin Coskun et al., Ameboid cell motility: A model and inverse problem, with an application to live cell imaging data, Journal of Theoretical Biology (2006), doi:10.1016/j.jtbi.2006.07.025.

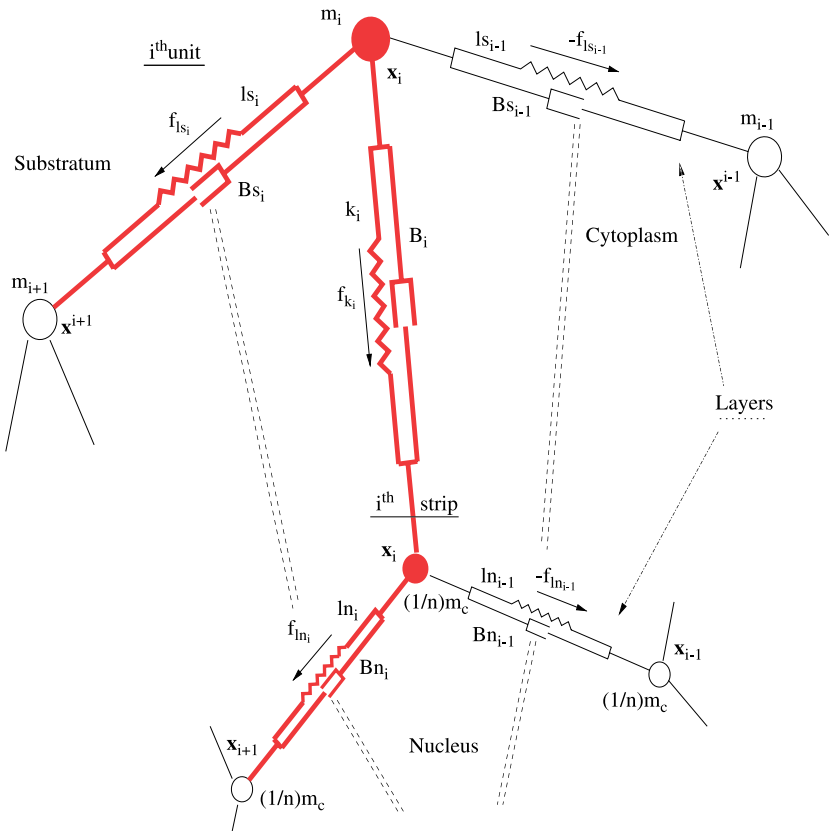

Fig. 1. The Ring Model diagram (*i*th unit—thick lines).

nucleus (see Fig. 1). A strip is defined to be the part of the cytoplasm along which a radial subunit lies, and the mass of each such strip is assumed to be a point mass at the membrane end of this subunit. The other ends of the subunits are connected to masses which are $1/n$ of the mass of the nucleus and are located at a radial distance from the center of the nucleus. The cell and nuclear membranes are also considered as circumferential subunits in series, each one connecting the ends of two consecutive radial subunits.

A computational unit of the model consists of a radial subunit, the corresponding cell, and nuclear membrane subunits on the positive side (counterclockwise) of the radial subunit, and the masses at either end of that radial subunit. We use the term 'layers' to mean the inner and outer boundaries of the ring structure.

The model can be used to approximate mechanical properties of the cell, like elasticity, viscosity, drag coefficient, etc. For example, the spring constants of the model (k, ln, ls) are linear approximations to the elasticity of the strips and the membranes. All springs are considered as being subject to a damping force due to the viscosity of the cytoplasm, and correspondingly the model parameters (B, Bn, Bs) are linear approximations to the viscosity of the strips. The combination of friction effects that the masses are subject to, due to the cell–substrate interaction and adhesion between the cell and substratum, is also incorporated in the model through the coefficients (Dn, Ds). In addition to the mechanical properties, the model may give some biophysical and chemical insights about the cell using the correspondence given below:

Overall, it is evident that the mechanical changes and motility of cells are due to some biochemical alterations in the cell. This strong relation between motility and the biochemical structure of the cell implies that the investigation of the data through the inverse problem obtained under different chemical or physical conditions may provide a way to deduce some insight about the chemical and biophysical alterations in the cell.

Due to the heterogeneity of the cell, the subunits are assumed to have different features varying with spatial position, like effective spring constants, spring rest lengths, and damping coefficients. Also the masses are assumed to be different, as are the drag coefficients in space. All parameters are also assumed to vary as functions of time.

The radial springs are assumed to be linear aging springs (i.e. the effective spring constants of the springs vary as time elapses) to approximate the cytoskeletal filament dynamics, like bundling, networking, aggregation, or activation of the actomyosin complex. For membrane springs, this variation is considered as an approximation to the change in the surface tension.

In this model the equilibrium lengths of the radial springs are assumed to be able to change in time to approximate some other cytoskeletal dynamics like polymerization of the filaments. Similarly, this parameter stands for membrane growth and vesicle trafficking for the membranes.

Please cite this article as: Huseyin Coskun et al., Ameboid cell motility: A model and inverse problem, with an application to live cell imaging data, Journal of Theoretical Biology (2006), doi:10.1016/j.jtbi.2006.07.025.

In order to include the intracellular motion, mass relocation within the cell, and cell and nucleus growth in the model, the masses are allowed to change in time. For simplicity, conservation of mass is not included in the system of model equations. For local analysis, masses need to be redefined appropriately.

2.2. Application of the model to live cell imaging data

At some discrete time steps with a constant increment, the membrane ends and the nuclear ends of the radial subunits are determined. These data are used for the solution of the system of equations, Eq. (2.3), numerically. The solutions give us discrete functions determined at these time steps for parameters: equilibrium lengths, spring constants, damping coefficients, drag coefficients, and the masses. By interpolation techniques, the values of these functions can be approximated at any time within the model limits to get an approximation for the continuous change in the values of the model parameters.

The Large-Scale Digital Cell Analysis System (LSDCAS) technique was used to get the data for application of the Ring Model. LSDCAS is designed to analyse large numbers of cells under a variety of experimental conditions, and is used in general for quantitation of cell motility. It is an automated microscope system capable of monitoring on the order of 1000 microscope fields over time intervals of up to one month. It is also used in the study of alterations in cell motility associated with metastasis, determination of the fate of cells which overproduce pro-oxidants, automatic determination of the mode for cell death following exposure to cytotoxic agents, and real-time fluorescence-based analysis. For further information, see the recent articles by the designers of this technique: Ianzini and Mackey (2002) and Ianzini et al. (2002).

Time-lapse sequences were obtained at 10-min intervals (i.e. $t = 0, 10, 20, \ldots, 60$ min). The number of radial subunits is assumed arbitrarily to be 50 for this application. At each time step, the positions of the point masses are hand-segmented approximately according to the number of radial subunits determined using geometry of the 2-D projection of the cell (see Fig. 3). Since the cells are moving slowly, the geometry of the projection is a strong indicator of the change in the position of a mass point from one time step to another. These masses are assumed to be cell and nuclear membrane ends of the radial subunits. These positions are used to solve the inverse problem. In Fig. 2 positions of the fifth and 24th units through time are shown. Both in Figs. 2 and 3 the dotted lines are the initial positions (i.e. $t = 0$ min) of the membranes and the solid lines are the final positions (i.e. $t = 60$ min).

After an introduction of the model equations, our main objective will be to illustrate that it is possible to extract the temporal evolution of the model parameters by fitting the model to data for the evolution of the inner and outer layers of the cell.

In the Ring Model, the SI unit system is used (see Table 1 and note that the units given in the table are for scaled parameters as explained in the next section).

2.3. The model equations

For a simple 1-D model of a spring with free ends which is subject to damping, by assuming that there are two masses m_1 and m_2 attached to the ends of the spring which are positioned at x_1 and x_2, respectively, the model equations become:

$$m_1\ddot{x}_1 = -k\left((x_1 - x_2) - K\frac{x_1 - x_2}{|x_1 - x_2|}\right) - B(\dot{x}_1 - \dot{x}_2) - D_1\dot{x}_1,$$

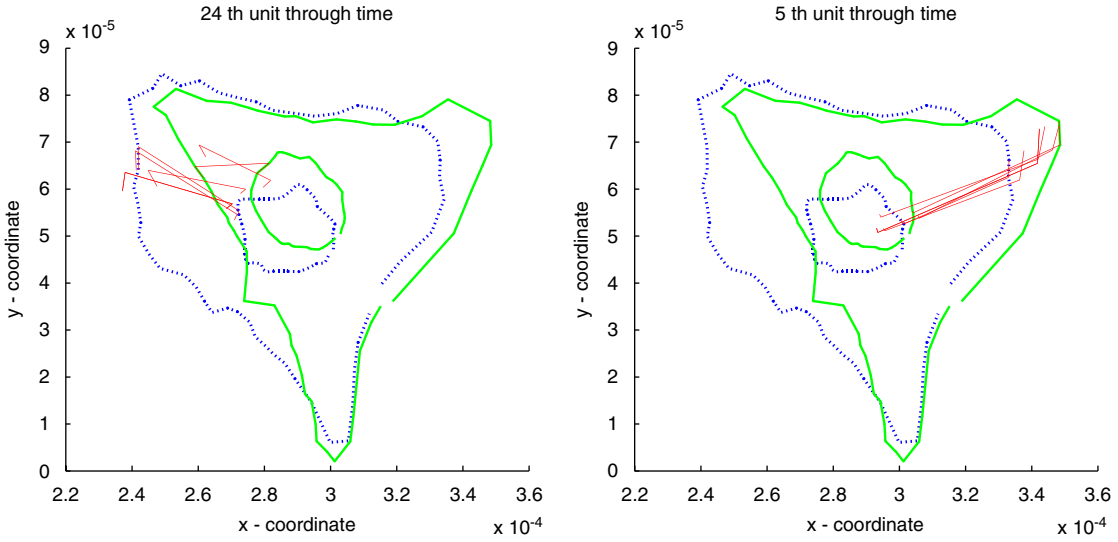

Fig. 2. Fifth and 24th units at different time steps (see text for explanation).

Please cite this article as: Huseyin Coskun et al., Ameboid cell motility: A model and inverse problem, with an application to live cell imaging data, Journal of Theoretical Biology (2006), doi:10.1016/j.jtbi.2006.07.025.

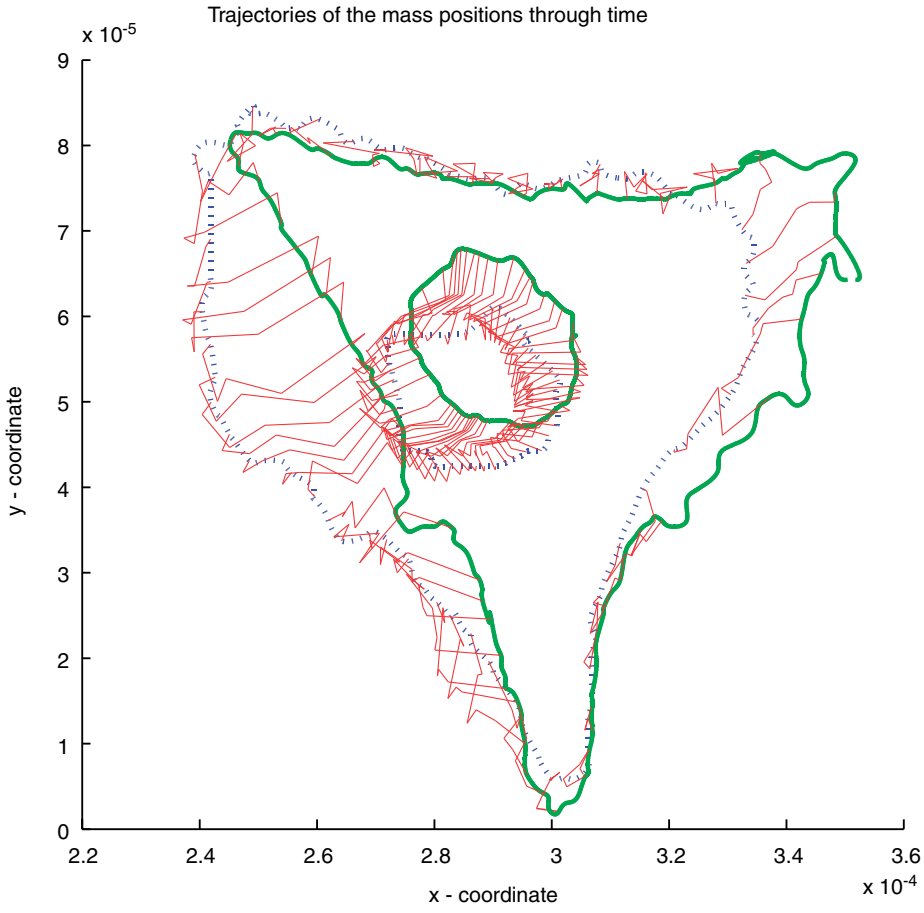

Fig. 3. Trajectories of the membrane ends of radial subunits.

Table 1
The scaled model parameters and their units (SI)

p	Stand for	Units
k_i	Radial spring constants	$1/s^2$
K_i	Radial spring rest lengths	m/kg
B_i	Damping constants for the radial springs	1/s
ls_i	Cell membrane spring constants	$1/s^2$
Ls_i	Cell membrane spring rest lengths	m/kg
Bs_i	Damping constants for the cell membrane springs	1/s
Ds_i	Drag coefficients at the cell membrane ends of the radial springs	1/s
ln_i	Nuclear membrane spring constants	$1/s^2$
Ln_i	Nuclear membrane spring rest lengths	m/kg
Bn_i	Damping constants for the nuclear membrane springs	1/s
Dn_i	Drag coefficients at the nuclear ends of the radial springs	1/s
m_i	Masses at the membrane ends of the radial springs	–
m_c	Mass of the nucleus	kg

$$m_2\ddot{x}_2 = k\left((x_1 - x_2) - K\frac{x_1 - x_2}{|x_1 - x_2|}\right) + B(\dot{x}_1 - \dot{x}_2) - D_2\dot{x}_2,$$

where k is the spring constant, K is the rest length of the spring, B is the viscosity coefficient, and D_i are drag coefficients.

For n radial subunits involved in the model, the positions of the membrane ends of the radial subunits will be denoted by $\mathbf{x}^i$ and those of nuclear ends by $\mathbf{x}_i$ where $\mathbf{x}^i = (x^i, y^i)$ and $\mathbf{x}_i = (x_i, y_i)$.

The basic idea is that if we can find the equation of motion for all motile points, the solution of that system will give us the movement of the cell.

There are three forces acting on the masses at the membrane ends of the radial subunits, two coming from the neighboring membrane subunits, and one due to the radial subunits (see Fig. 1). So by Newton's second law, $\mathbf{F} = m\mathbf{a}$, the equation of motion for the membrane ends and the nuclear ends of the subunits, respectively, becomes as follows:

$$\begin{aligned} &\mathbf{f}_{ln_i} - \mathbf{f}_{ln_{i-1}} - \mathbf{f}_{k_i} - Dn_i\dot{\mathbf{x}}_i = \frac{m_c}{n}\ddot{\mathbf{x}}_i, \\ &\mathbf{f}_{ls_i} - \mathbf{f}_{ls_{i-1}} + \mathbf{f}_{k_i} - Ds_i\dot{\mathbf{x}}^i = m_i\ddot{\mathbf{x}}^i. \end{aligned} \tag{2.1}$$

Here $\mathbf{f}_s$ is the force due to the subunit with spring constant s, m_c is the mass of the nucleus, m_i are the point masses at the cell membrane ends of the radial subunits, Dn_i, Ds_i are drag coefficients that the point masses at the nuclear and cell membrane ends of radial subunits are subject to, respectively.

Therefore, we have a system, Eq. (2.1), of $4n$ nonlinear second-order ordinary differential equations (ODEs)

Please cite this article as: Huseyin Coskun et al., Ameboid cell motility: A model and inverse problem, with an application to live cell imaging data, Journal of Theoretical Biology (2006), doi:10.1016/j.jtbi.2006.07.025.

(coming from the equation of motion for each component of the positions $\mathbf{x}^i$, $\mathbf{x}_i$). The system and the corresponding initial/boundary conditions constitute the system for the forward problem, that is, for a given set of parameters the solution of the system, Eq. (2.1), gives the position of the cell at any time.

More specifically, the forces due to the nuclear subunits, membrane subunits, and radial subunits, respectively, are:

$$\begin{aligned}
\mathbf{f}_{ln_i} = & -ln_i\left[(\mathbf{x}_i-\mathbf{x}_{i+1})-Ln_i\left(\frac{\mathbf{x}_i-\mathbf{x}_{i+1}}{|\mathbf{x}_i-\mathbf{x}_{i+1}|}\right)\right]\\
& -Bn_i[(\dot{\mathbf{x}}_i-\dot{\mathbf{x}}_{i+1})],\\
\mathbf{f}_{ls_i} = & -ls_i\left[(\mathbf{x}^i-\mathbf{x}^{i+1})-Ls_i\left(\frac{\mathbf{x}^i-\mathbf{x}^{i+1}}{|\mathbf{x}^i-\mathbf{x}^{i+1}|}\right)\right]\\
& -Bs_i[(\dot{\mathbf{x}}^i-\dot{\mathbf{x}}^{i+1})],\\
\mathbf{f}_{k_i} = & -k_i\left[(\mathbf{x}^i-\mathbf{x}_i)-K_i\left(\frac{\mathbf{x}^i-\mathbf{x}_i}{|\mathbf{x}^i-\mathbf{x}_i|}\right)\right]\\
& -B_i[(\dot{\mathbf{x}}^i-\dot{\mathbf{x}}_i)].
\end{aligned}\tag{2.2}$$

For simplicity the following substitutions are done:

$$\mathbf{u}_{ni}=\mathbf{x}_i-\mathbf{x}_{i+1},\quad \mathbf{v}_{ni}=\frac{\mathbf{x}_i-\mathbf{x}_{i+1}}{|\mathbf{x}_i-\mathbf{x}_{i+1}|},\quad \mathbf{w}_{ni}=\dot{\mathbf{x}}_i-\dot{\mathbf{x}}_{i+1},$$

$$\mathbf{u}_{si}=\mathbf{x}^i-\mathbf{x}^{i+1},\quad \mathbf{v}_{si}=\frac{\mathbf{x}^i-\mathbf{x}^{i+1}}{|\mathbf{x}^i-\mathbf{x}^{i+1}|},\quad \mathbf{w}_{si}=\dot{\mathbf{x}}^i-\dot{\mathbf{x}}^{i+1},$$

$$\mathbf{u}_i=\mathbf{x}^i-\mathbf{x}_i,\quad \mathbf{v}_i=\frac{\mathbf{x}^i-\mathbf{x}_i}{|\mathbf{x}^i-\mathbf{x}_i|},\quad \mathbf{w}_i=\dot{\mathbf{x}}^i-\dot{\mathbf{x}}_i.$$

For the inverse problem $\mathbf{u}_{ni}$, $\mathbf{v}_{ni}$, $\mathbf{w}_{ni}$, $\mathbf{u}_{si}$, $\mathbf{v}_{si}$, $\mathbf{w}_{si}$, $\mathbf{u}_i$, $\mathbf{v}_i$, $\mathbf{w}_i$ are all known constant vectors, since in this case the positions are provided and parameters are unknown. In this setting $\mathbf{x}_{i+1}=\mathbf{x}_1$ (respectively, $\mathbf{x}^{i+1}=\mathbf{x}^1$) for $i=n$ and $\mathbf{x}_{i-1}=\mathbf{x}_n$ (respectively, $\mathbf{x}^{i-1}=\mathbf{x}^n$) for $i=1$. As a result, we have the following nonlinear system of equations to solve for the parameters of the model (see Table 1) where the position vectors are known and their derivatives with respect to time approximated by using finite difference formulas:

$$\begin{aligned}
\frac{m_c}{n}\ddot{\mathbf{x}}_i = & -(\mathbf{u}_{ni}ln_i-\mathbf{v}_{ni}ln_iLn_i+\mathbf{w}_{ni}Bn_i)\\
& +(\mathbf{u}_{n(i-1)}ln_{i-1}-\mathbf{v}_{n(i-1)}ln_{i-1}Ln_{i-1}+\mathbf{w}_{n(i-1)}Bn_{i-1})\\
& +(\mathbf{u}_ik_i-\mathbf{v}_ik_iK_i+\mathbf{w}_iB_i)-Dn_i\dot{\mathbf{x}}_i,\\
m_i\ddot{\mathbf{x}}^i = & -(\mathbf{u}_{si}ls_i-\mathbf{v}_{si}ls_iLs_i+\mathbf{w}_{si}Bs_i)\\
& +(\mathbf{u}_{s(i-1)}ls_{i-1}-\mathbf{v}_{s(i-1)}ls_{i-1}Ls_{i-1}+\mathbf{w}_{s(i-1)}Bs_{i-1})\\
& -(\mathbf{u}_ik_i-\mathbf{v}_ik_iK_i+\mathbf{w}_iB_i)-Ds_i\dot{\mathbf{x}}_i,
\end{aligned}\tag{2.3}$$

where $i=1,\ldots,n$.

There is only one term with nonlinearity at each force in Eq. (2.2) and it comes from the product of spring constants and rest lengths. Since each pair, for example, $(k_i,K_i)\leftrightarrow(k_i,k_iK_i)$ uniquely determines the other (except for the trivial case which lacks physical meaning), the product can be renamed as $k_iK_i\to K_i$ to linearize the system, Eq. (2.3). Each equation is also scaled by the mass of the nucleus to get

$$\begin{aligned}
\frac{1}{n}\ddot{\mathbf{x}}_i = & -(\mathbf{u}_{ni}ln_i-\mathbf{v}_{ni}Ln_i+\mathbf{w}_{ni}Bn_i)\\
& +(\mathbf{u}_{n(i-1)}ln_{i-1}-\mathbf{v}_{n(i-1)}Ln_{i-1}\\
& +\mathbf{w}_{n(i-1)}Bn_{i-1})+(\mathbf{u}_ik_i-\mathbf{v}_iK_i+\mathbf{w}_iB_i)-Dn_i\dot{\mathbf{x}}_i,\\
0 = & -m_i\ddot{\mathbf{x}}^i-(\mathbf{u}_{si}ls_i-\mathbf{v}_{si}Ls_i+\mathbf{w}_{si}Bs_i)\\
& +(\mathbf{u}_{s(i-1)}ls_{i-1}-\mathbf{v}_{s(i-1)}Ls_{i-1}+\mathbf{w}_{s(i-1)}Bs_{i-1})\\
& -(\mathbf{u}_ik_i-\mathbf{v}_iK_i+\mathbf{w}_iB_i)-Ds_i\dot{\mathbf{x}}_i,
\end{aligned}\tag{2.4}$$

where now

$$ln_i\coloneqq\frac{ln_i}{m_c},\quad Ln_i\coloneqq\frac{ln_i\,Ln_i}{m_c},\quad Bn_i\coloneqq\frac{Bn_i}{m_c},$$
$$m_i\coloneqq\frac{m_i}{m_c},\quad i=1,\ldots,n,$$

etc. The vector of unknown parameters can be written as (see Table 1):

$$\mathbf{p}=[ln,Ln,Bn,k,K,B,Dn,ls,Ls,Bs,Ds,m]^{\mathrm{T}},$$

where the subvectors are, for example, like $ln=[ln_1,\ldots,ln_i,\ldots,ln_n]$.

Using submatrices, for example,

$$\bar{k}=\begin{bmatrix}
u_1^x & \ldots & 0 & \ldots & 0\\
u_1^y & \ldots & 0 & \ldots & 0\\
\vdots & \vdots & \vdots & \vdots & \vdots\\
0 & \ldots & u_j^x & \ldots & 0\\
0 & \ldots & u_j^y & \ldots & 0\\
\vdots & \vdots & \vdots & \vdots & \vdots\\
0 & \ldots & 0 & \ldots & u_n^x\\
0 & \ldots & 0 & \ldots & u_n^y
\end{bmatrix},$$

$$\bar{ls}=\begin{bmatrix}
-u_{s1}^x & \ldots & 0 & \ldots & u_{sn}^x\\
-u_{s1}^y & \ldots & 0 & \ldots & u_{sn}^y\\
u_{s1}^x & \ldots & 0 & \ldots & 0\\
u_{s1}^y & \ldots & 0 & \ldots & 0\\
\vdots & \vdots & \vdots & \vdots & \vdots\\
0 & \ldots & -u_{sj}^x & \ldots & 0\\
0 & \ldots & -u_{sj}^y & \ldots & 0\\
0 & \ldots & u_{sj}^x & \ldots & 0\\
0 & \ldots & u_{sj}^y & \ldots & 0\\
\vdots & \vdots & \vdots & \vdots & \vdots\\
0 & \ldots & 0 & \ldots & -u_{sn}^x\\
0 & \ldots & 0 & \ldots & -u_{sn}^y
\end{bmatrix},$$

Please cite this article as: Huseyin Coskun et al., Ameboid cell motility: A model and inverse problem, with an application to live cell imaging data, Journal of Theoretical Biology (2006), doi:10.1016/j.jtbi.2006.07.025.

$\bar{0}$, etc., which are $2n \times n$ matrices, we have the following coefficient matrix:

$$\mathbf{U} = \begin{bmatrix} \bar{l}n & \bar{L}n & \bar{B}n & \bar{k} & \bar{K} & \bar{B} & \bar{D}n & \bar{0} & \bar{0} & \bar{0} & \bar{0} & \bar{0} \\ \bar{0} & \bar{0} & \bar{0} & -\bar{k} & -\bar{K} & -\bar{B} & \bar{0} & \bar{l}s & \bar{L}s & \bar{B}s & \bar{D}s & \bar{M} \end{bmatrix}.$$

The matrix $\mathbf{U}$ is $4n \times 12n$ and then the system, Eq. (2.3), which is different for each time step, turns out to be

$$\mathbf{Up} = \mathbf{d}, \tag{2.5}$$

where

$$\mathbf{d} = \left[\frac{\ddot{x}_1}{n}, \frac{\ddot{y}_1}{n}, \ldots, \frac{\ddot{x}_i}{n}, \frac{\ddot{y}_i}{n}, \ldots, \frac{\ddot{x}_n}{n}, \frac{\ddot{y}_n}{n}, 0, 0, \ldots, 0, 0, \ldots, 0, 0 \right]^{\mathrm{T}}.$$

Clearly, the system is underdetermined. To make it exactly determined it is assumed that the parameters are constant locally in time for three consecutive time steps. This is a reasonable assumption because of the slow speed of the cell. The slow motion implies that the changes in the motility-related parameters are negligible.

It should be also noted that the derivatives are approximated by difference formulas after a piecewise interpolation of the original data using splines along the time axis to get finer results. In the reformulation of the inverse problem as a matrix equation, Eq. (2.5), both the coefficient matrix and the vector on the right-hand side are dependent on the first and/or second derivatives. Therefore, the coefficient matrix is ill-conditioned with a quite high condition number for rough approximations to the derivatives. It is necessary to have finer approximations to the derivatives for a better solution, as it makes the condition number smaller. Iterative methods, and even regularization techniques, do not work with this highly ill-conditioned system.

3. Results

The Ring Model is applied to both an arbitrary set of simulated data and live cell imaging data. The former application shows the reliability of the model. The corresponding results are as follows.

3.1. Results obtained from an arbitrary set of simulated data

A Matlab program was coded for simulation of a crawling cell movement (forward problem) using the system, Eq. (2.1), to check the reliability of the model. For the simulation, a set of arbitrarily pre-determined parameters was input and the code solved the second-order nonlinear ODE system, Eq. (2.3), of $4n$ equations and animated it. The solutions were the positions of the spring ends at the specified times. Then, in the second step, this simulated data set (positions) was used to solve the inverse problem. The code for the inverse problem provides the exact solution (the pre-determined parameter set) up to around $1e-22$ accuracy. This shows that the method developed for the solution of the model and the inverse problem is working for arbitrary data sets.

3.2. Results obtained from live cell imaging data

The exact solution to the inverse problem for real data (live cell imaging data, as explained in Section 2.2 and visualized on the graphs of Figs. 3 and 2) has some negative values for parameters. Negative elasticity and viscosity were observed, and since around 30% of the parameter values for mass and spring rest lengths were also negative, an optimization routine was used to restrict solutions to the positive cone of real values. The built-in function *lsqlin* of Matlab was used to get those results presented here (see Figs. 4 and 5 and Section 4). The results are accurate up to around $1e-15$ residual norm.

In the figures, subgraphs are plotted without an x-label for clarity of the whole picture and parameters are labeled at the upper right corner of the corresponding graphs. The x-axis for each graph is the time $t = 0, 1, 2, \ldots, 3600$ s. Note also that the results are the solutions for the scaled parameters except the rest lengths (K_i, Ln_i, Ls_i) because unscaled parameters can be and are calculated for the rest lengths by the ratio K_i/k_i, etc. of the corresponding scaled parameters.

The following observations mostly related to the mechanical properties of the cell can be made by just analysing the graphs.

First recalling that the solutions for the unscaled rest lengths $(K_i, Ln_i, Ls_i, i = 5, 24)$ are presented, one can easily check that these values are consistent with the size of the cell (compare Figs. 3, 4, and 5). Namely, the order of magnitude of the cell size is $1e-4 \times 1e-4$ and those of the radial spring rest lengths, K_i, cell membrane spring rest lengths, Ls_i, nuclear membrane spring rest lengths, Ln_i, are $1e-5, 1e-6, 1e-6$, respectively, and they are consistent with each other.

From Fig. 2 it is clear that the cell is expanding around strip 5 and shrinking around strip 24. The results reflect this phenomenon: the rest length K_5 of radial subunit 5 is increasing and the rest length K_{24} of radial subunit 24 is decreasing. Moreover, the same pattern for the change of masses is valid as expected; m_5 is increasing and m_{24} is decreasing through time. Similarly, while the spring constant k_5 of radial subunit 5 is oscillating with a small overall decrease, the spring constant k_{24} of radial subunit 24 is increasing and reflects the elastic behavior of the contraction.

Looking overall at the graphs presented, one can realize that the spring constants are mostly increasing and the rest lengths, viscosity, and drag coefficients are decreasing for both units 5 and 24. That shows that the cell is maximizing force generation at the protruding and contracting sites.

Similar analysis can be done for other subunits of units 5 and 24 and the other units as well. One can see that the results and the correspondence given in Section 2.1, for example polymerization at the leading edge and increasing

Please cite this article as: Huseyin Coskun et al., Ameboid cell motility: A model and inverse problem, with an application to live cell imaging data, Journal of Theoretical Biology (2006), doi:10.1016/j.jtbi.2006.07.025.

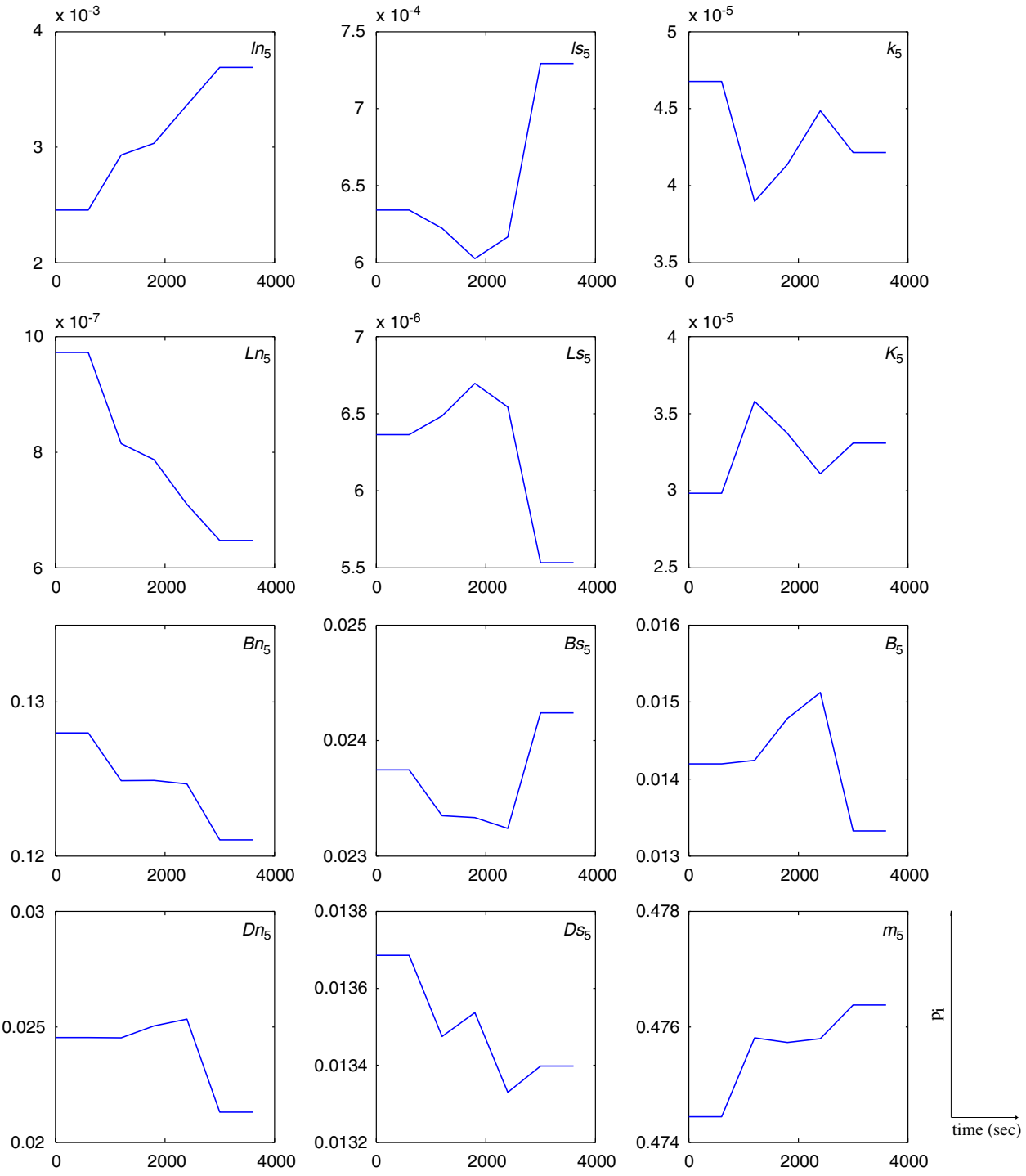

Fig. 4. Solutions of the parameters for unit 5 (see Fig. 2).

K_5, activation of the actomyosin complex to create contractility and increasing k_{24}, etc., appear to be consistent.

4. Discussion

The model, its implementation, results, and future steps are discussed in the following subsections.

4.1. The model

In this article, the primary aim was to introduce the Ring Model, show its validity, and also provide an example of its application using a set of real data.

It is shown that the model achieves quite high accuracy in finding the exact solution for the inverse problem, as explained in the previous section, for arbitrary data sets

Please cite this article as: Huseyin Coskun et al., Ameboid cell motility: A model and inverse problem, with an application to live cell imaging data, Journal of Theoretical Biology (2006), doi:10.1016/j.jtbi.2006.07.025.

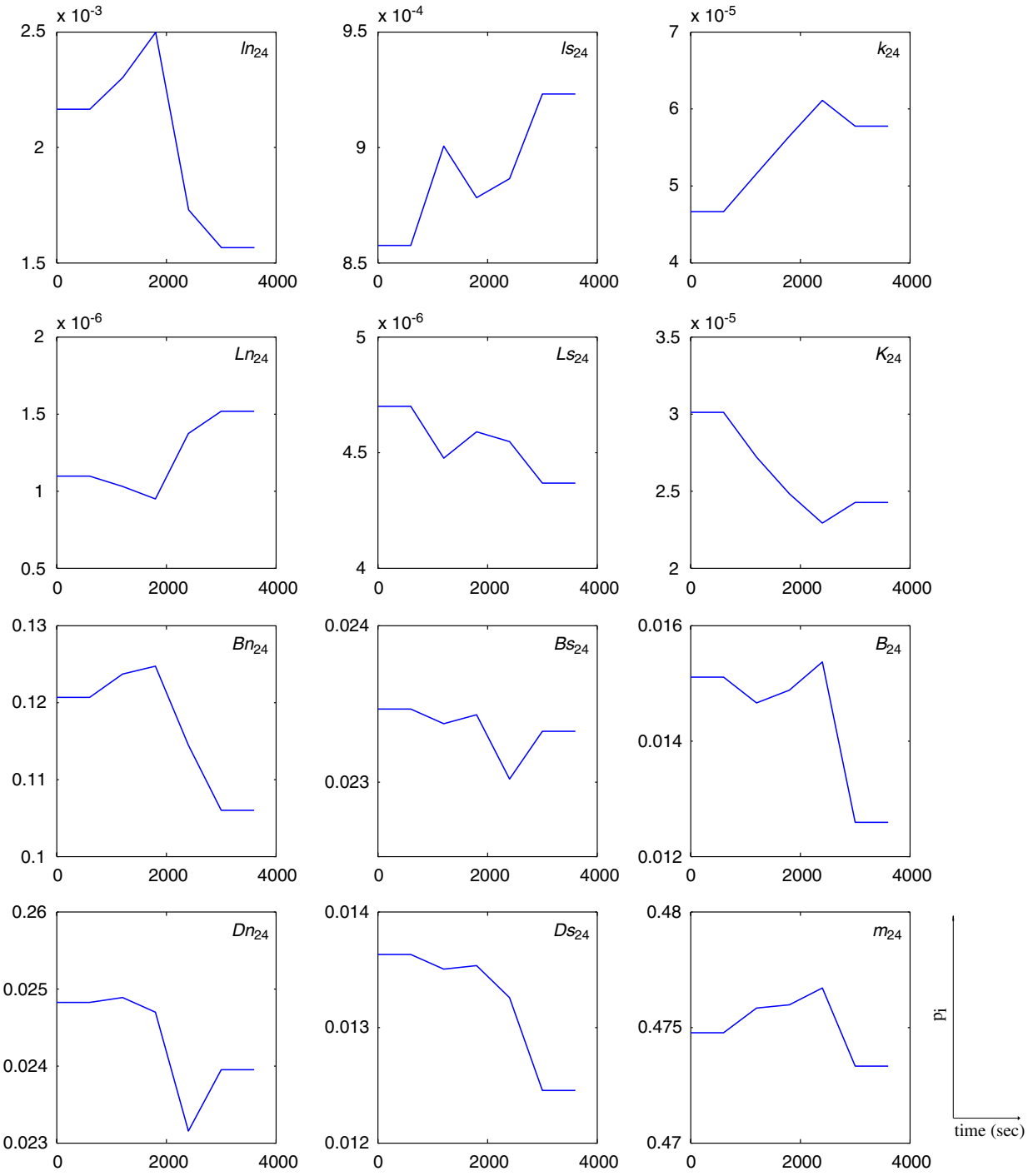

Fig. 5. Solutions of the parameters for unit 24 (see Fig. 2).

obtained from the implementation of the forward problem.

Application of the model to a set of live cell imaging data justified the correspondence set forth in Section 2.1 between the model setting and known related biophysical and mechanochemical explanations up to some level. This correspondence, after more experimental justification, can be used for analysis of different applications.

Any cross-section of the cell through the nucleus in 3-D reduces to a 2-D flat surface and therefore the model can be applied. In order to obtain local mechanical characteristics of the cell rather than global approximations, more layers can be assumed within the cell other than the membranes. Since it may be expensive in terms of numerical calculations, a pair of layers (ring) within the cell, not necessarily the membranes, can be assumed instead. As the layers of the ring get closer, finer results can be obtained for sufficiently large n.

The model can also be used for estimation or measurement of chemical and biophysical changes at important

Please cite this article as: Huseyin Coskun et al., Ameboid cell motility: A model and inverse problem, with an application to live cell imaging data, Journal of Theoretical Biology (2006), doi:10.1016/j.jtbi.2006.07.025.

steps or processes during the life cycle of the cell, such as growth, division, death, etc. It may lead to some useful relations among the model parameters which might be valid biologically as well.

4.2. Numerical computations and the data

We use the quasi-steady-state approach in the solution of the model equations of the inverse problem. That is, for the numerical computations, parameters are considered to be constant locally in time, but they are treated as functions of time globally. This approach simplifies the model to its present form of a nonlinear ODE system instead of a nonlinear partial differential equation (PDE) system.

For the data set used in this paper, the step size (10 min) for time increments seems to be big. However, this choice is actually suitable for the case of slowly moving cell. For slowly moving cells, as mentioned above, it is reasonable to think that motility-related parameters are also altering slowly which constitute a reason for using quasi-steady-state method.

4.3. Future steps and improvements

In order to justify the correspondence set forth in Section 2.1 and also to get biochemical insights about the cell using the Ring Model, or to derive conclusions about the effect of the medium, different measurements under different chemical conditions (like different pH level of substratum, chemicals causing chemotaxis, temperature, etc.) are needed. Time and space do not allow the presentation in the present article of an application of the model to these different experimental settings, and thus we leave further discussion, interpretation, biophysical, and mechanochemical implications to a larger article, which is in progress.

We primarily focused on the inverse problem, and for the inverse problem the only necessary information is the position set of the point masses. For that reason, the forward problem is left relatively simple, and cell-to-cell adhesion and directed motion, for example, are not considered. The model will be improved in a way that reproduces the whole movement of the cell by incorporating some other aspects of the cell movement. Mathematical formulations of the properties of integrin proteins, for example, can allow us to include directed motion into the model (see, for example, Cox and Huttenlocher, 1998; Munevar et al., 2001; Palecek et al., 1996, 1997; Verkhovsky et al., 1999).

The subunits used for modeling are simple Voigt solid elements. Some other combinations (see, for example, Bray's suggestion (2001) for a different unit design) of Boltzmann elements and contractile elements can be assumed and may lead to finer representation of the cytoskeletal dynamics. Such improvements, together with fluid dynamics involvement, will be discussed in a later work.

The restriction on the parameters as being constant locally in time will be removed. The system for parameters as functions of space and time has already been formulated using the Lagrangian, and it is observed that the PDE system obtained reduces to the ODE system, Eq. (2.3), for constant parameters. This is not only confirmation of the model, Eq. (2.3), but also leads to some energy considerations and gives us the ability to use the terminology and techniques of variational methods.

4.4. Limitations of the model

The major difficulty in the application of the Ring Model is getting the positions of point masses accurately through time. For this paper, the positions of the masses are determined approximately by a careful analysis of the graphs obtained from the real data. Using fluorescence microscopy or some other advanced techniques to determine the positions of the point masses assumed to be located at cell and nuclear membranes, however, may lead to finer results. More precise, rather than approximate, determination of the mass points, and a sensitivity analysis of the model (i.e. how the different choice of mass points affects the result), will be studied in a separate paper.

Acknowledgments

This work was supported by Grant CA/GM94801 awarded by the National Institutes of Health, a Special Opportunity award from the Whitaker Foundation, and University of Iowa.

Yi Li is supported in part by the National Science Foundation of China (10471052) and by the Xiao-Xiang Funds of the Hunan Normal University, China.

The authors are also indebted to Ms. Elizabeth A. Kosmacek for skillful analysis of the LSDCAS live cell imaging data.

References

Abercrombie, M., 1980. The Croonian lecture, 1978: the crawling movement of metazoan cells. Proc. R. Soc. London B: Biol. Sci. 207, 129–147.

Alberts, B., Johnson, A., Lewis, J., Raff, M., Roberts, K., Walter, P., 2002. Molecular Biology of the Cell. Garland, New York.

Alt, W., Dembo, M., 1999. Cytoplasm dynamics and cell motion: two-phase flow models. Math. Biosci. 156, 207–228 (special issue entitled epidemiology, cellular automata, and evolution).

Bausch, A.R., Moller, W., Sackmann, E., 1999. Measurement of local viscoelasticity and forces in living cells by magnetic tweezers. Biophys. J. 76, 573–579.

Bottino, D., Mogilner, A., Roberts, T., Stewart, M., Oster, G., 2002. How nematode sperm crawl. J. Cell Sci. 115, 367–384.

Bray, D., 2001. Cell Movements. Garland, New York.

Caille, N., Thoumine, O., Tardy, Y., Meister, J.J., 2002. Contribution of the nucleus to the mechanical properties of endothelial cells. J. Biomech. 35 (2), 177–188.

Chicurel, M., 2002. Cell migration research is on the move. Science 295, 606–609.

Please cite this article as: Huseyin Coskun et al., Ameboid cell motility: A model and inverse problem, with an application to live cell imaging data, Journal of Theoretical Biology (2006), doi:10.1016/j.jtbi.2006.07.025.

Coskun, H., 2006a. A continuum model with free boundary formulation and the inverse problem for ameboid cell motility. Preprint.

Coskun, H., 2006b. Mathematical models for cell motility and model-based inverse problems. PhD Thesis, Department of Mathematics, University of Iowa.

Cox, E., Huttenlocher, A., 1998. Regulation of integrin-mediated adhesion during cell migration. Microsc. Res. Tech. 43, 412–419.

Defilippi, P., Olivo, C., Venturino, M., Dolce, L., Silengo, L., Tarone, G., 1999. Actin cytoskeleton organization in response to integrin-mediated adhesion. Microsc. Res. Tech. 47, 67–78.

DiMilla, P.A., Barbee, K., Lauffenburger, D.A., 1991. Mathematical model for the effects of adhesion and mechanics on cell migration speed. Biophys. J. 60, 15–37.

Dong, C., Skalak, R., 1992. Leukocyte deformability: finite-element modeling of large viscoelastic deformation. J. Theor. Biol. 158, 173–193.

Feneberg, W., Westphal, M., 2001. Dictyostelium cells' cytoplasm as an active viscoplastic body. Eur. Biophys. J. 30, 284–294.

Gracheva, M.E., Othmer, H.G., 2004. A continuum model of motility in ameboid cells. Bull. Math. Biol. 66, 167–193.

Heidemann, S.R., Kaech, S., Buxbaum, R.E., Matus, A., 1999. Direct observations of the mechanical behaviors of the cytoskeleton in living fibroblasts. J. Cell Biol. 145, 109–122.

Ianzini, F., Mackey, M.A., 2002. Development of the large scale digital cell analysis system. Radiat. Prot. Dosimetry 99, 289–293.

Ianzini, F., Bresnahan, L., Wang, L., Anderson, K., Mackey, M.A., 2002. The Large Scale Digital Cell Analysis System and its use in the quantitative analysis of cell populations. In: Dittmar, A., Beebe, E. (Eds.), Second Annual International IEEE-EMB Special Topic Conference on Microtechnologies in Medicine and Biology (Madison, WI, 2002), IEEE, Piscataway, NJ, pp. 470–475.

Karcher, H., Lammerding, J., Huang, H., Lee, R.T., Kamm, R.D., Kaazempur-Mofrad, M.R., 2003. A three-dimensional viscoelastic model for cell deformation with experimental verification. Biophys. J. 85, 3336–3349.

Kaverina, I., Krylyshkina, O., Small, J.V., 2002. Regulation of substrate adhesion dynamics during cell motility. Int. J. Biochem. Cell Biol. 34, 746–761.

Lauffenburger, D., Horwitz, A., 1996. Cell migration: a physically integrated molecular process. Cell 84, 359–369.

MacKintosh, F.C., 1998. Theoretical models of viscoelasticity of actin solutions and the actin cortex. Biol. Bull. 194, 351–353.

Marella, S.V., Udaykumar, H.S., 2004. Computational analysis of the deformability of leukocytes modeled with viscous and elastic structural components. Phys. Fluids 16 (2), 244–264.

McGarry, J.G., Klein–Nulend, J., Mullender, M.G., Prendergast, P.J., 2004. A comparison of strain and fluid shear stress in stimulating bone cell responses—a computational and experimental study. FASEB J. 18 (15).

Mitchison, T.J., Cramer, L.P., 1996. Actin-based cell motility and cell locomotion. Cell 84, 371–379.

Mogilner, A., Edelstein-Keshet, L., 2002. Regulation of actin dynamics in rapidly moving cells: a quantitative analysis. Biophys. J. 83, 1237–1258.

Mogilner, A., Verzi, D.W., 2003. A simple 1-D physical model for the crawling nematode sperm cell. J. Stat. Phys. 110, 1169–1189.

Mogilner, A., Marland, E., Bottino, D., 2000. A minimal model of locomotion applied to the steady gliding movement of fish keratocyte cells. In: Maini, P.K., Othmer, H.G. (Eds.), Mathematical Models for Biological Pattern Formation, The IMA Volumes in Mathematics and its Applications, Frontiers in Application of Mathematics, vol. 121. Springer, New York, pp. 269–294.

Munevar, S., Wang, Y., Dembo, M., 2001. Traction force microscopy of migrating normal and H-ras transformed 3T3 fibroblasts. Biophys. J. 80, 1744–1757.

Palecek, S.P., Schmidt, C.E., Lauffenburger, D.A., Horwitz, A.F., 1996. Integrin dynamics on the tail region of migrating fibroblasts. J. Cell Sci. 109 (Part 5), 941–952.

Palecek, S.P., Loftus, J.C., Ginsberg, M.H., Lauffenburger, D.A., Horwitz, A.F., 1997. Integrin–ligand binding properties govern cell migration speed through cell–substratum adhesiveness. Nature 385, 537–540.

Palsson, E., Othmer, H.G., 2000. A model for individual and collective cell movement in *Dictyostelium discoideum*. Proc. Natl Acad. Sci. USA 97, 10448–10453.

Schmid-Schönbein, G., Kosawada, T., Skalak, R., Chien, S., 1995. Membrane model of endothelial cells and leukocytes: a proposal for the origin of a cortical stress. J. Biomech. Eng. 117, 171–178.

Small, J.V., 1989. Microfilament-based motility in non-muscle cells. Curr. Opin. Cell Biol. 1, 75–79.

Sultan, C., Stamenovic, D., Ingber, D.E., 2004. A computational tensegrity model predicts dynamic rheological behaviors in living cells. Ann. Biomed. Eng. 32 (4), 520–530.

Theriot, J., Mitchison, T., 1991. Actin microfilament dynamics in locomoting cells. Nature 352, 126–131.

Verkhovsky, A.B., Svitkina, T.M., Borisy, G.G., 1999. Self-polarization and directional motility of cytoplasm. Curr. Biol. 9, 11–20.

Yanai, M., Butler, J.P., Suzuki, T., Kanda, A., Kurachi, M., Tashiro, H., Sasaki, H., 1999. Intracellular elasticity and viscosity in the body, leading, and trailing regions of locomoting neutrophils. Am. J. Physiol. 277, C432–C440.

Yanai, M., Butler, J.P., Suzuki, T., Sasaki, H., Higuchi, H., 2004. Regional rheological differences in locomoting neutrophils. Am. J. Physiol. Cell Physiol. 287, C603–C611.

Yeung, A., Evans, E., 1989. Cortical shell-liquid core model for passive flow of liquid-like spherical cells into micropipets. Biophys. J. 56, 139–149.

Please cite this article as: Huseyin Coskun et al., Ameboid cell motility: A model and inverse problem, with an application to live cell imaging data, Journal of Theoretical Biology (2006), doi:10.1016/j.jtbi.2006.07.025.